MATHEMATICAL BIOSCIENCES
AND ENGINEERING
Volume **11**, Number **1**, February **2014**

doi:10.3934/mbe.2014.11.125

pp. **125–138**

GENERATION OF SLOW PHASE-LOCKED OSCILLATION AND VARIABILITY OF THE INTERSPIKE INTERVALS IN GLOBALLY COUPLED NEURONAL OSCILLATORS

Ryotaro Tsuneki and Shinji Doi

Graduate School of Engineering, Kyoto University
Kyoto 615-8510, Japan

Junko Inoue

Faculty of Human Relation, Kyoto Koka Women's University
Kyoto 615-0882, Japan

Abstract. To elucidate how a biological rhythm is regulated, the extended (three-dimensional) Bonhoeffer-van der Pol or FitzHugh-Nagumo equations are employed to investigate the dynamics of a population of neuronal oscillators globally coupled through a common buffer (mean field). Interesting phenomena, such as extraordinarily slow phase-locked oscillations (compared to the natural period of each neuronal oscillator) and the death of all oscillations, are observed. We demonstrate that the slow synchronization is due mainly to the existence of "fast" oscillators. Additionally, we examine the effect of noise on the synchronization and variability of the interspike intervals. Peculiar phenomena, such as noise-induced acceleration and deceleration, are observed. The results herein suggest that very small noise may significantly influence a biological rhythm.

1. **Introduction.** In life, there are many oscillations and various rhythmic phenomena such as cardiac beats and circadian rhythms [10]. The interaction or coupling of numerous microscopic autonomously oscillatory elements with differing natural periods determines the macroscopic biological rhythm [20]. For instance, the sinoatrial node cells (cardiac pacemaker cells), which are located in the right atrium of the heart, are mutually coupled via electrical synapses called gap junctions and the electrical impulses (action potentials) generated by the pacemaker cells are propagated throughout the atrium. Abnormal biological rhythms, whether regular or irregular, cause serious diseases such as cardiac arrhythmia. Because the biological rhythm plays a crucial role in living organisms, analysis of its modulation mechanism leads to a deeper understanding of biological phenomena.

Biological phenomena have been frequently analyzed using mathematical models [1, 3, 8, 16]. In particular, a system of coupled oscillators has been employed for analysis of the rhythm modulation mechanism in life. These mathematical approaches are useful for conducting real physiological experiments and for developing treatment of diseases caused by abnormal rhythms. However, to our knowledge, the dynamics of a population of neuronal oscillators globally coupled through a common environment has yet to be investigated, although many studies have examined

2010 *Mathematics Subject Classification.* Primary: 92C20, 34C15; Secondary: 37N25.

Key words and phrases. Slow phase-locked oscillation, globally coupled system, neuronal oscillator, interspike interval.

such systems using other nonlinear oscillators (e.g., [15]). A neuronal oscillator has multiple time scales and is an example of a singularly perturbed system or relaxation oscillator. To examine how a biological rhythm is regulated, it is important to investigate how interactions between such neuronal oscillators generate a macroscopic rhythm. In a system of coupled oscillators, various complicated patterns of synchronous or asynchronous oscillations are observed. Such oscillations depend mainly on the network topology of the coupled system in general. In this paper, in order to focus on the effect of time scales of each oscillator, we would like to take the network topology as simple as possible. Thus, we analyze the dynamics of a population of neuronal oscillators globally coupled through a common buffer (mean field).

Hodgkin-Huxley (HH) equations are the typical neuron model to describe the generation of action potentials phenomenologically [13]. A globally coupled system of neuronal oscillators has been analyzed using these equations [21]. The system oscillated in a phase-locked state very slowly compared to the natural period of each neuronal oscillator or the firings were completely inhibited. These phenomena have not been observed in a coupled system of normal nonlinear oscillators, e.g., phase oscillators [17] and so on. Due to the complex dynamics of the HH equations, theoretical analysis is difficult, and the generation mechanism of these phenomena has yet to be clarified. To elucidate their generation mechanisms, these phenomena must be reproduced using simpler systems.

In this paper, a population of globally coupled neuronal oscillators is analyzed using the extended (three-dimensional) Bonhoeffer-van der Pol or FitzHugh-Nagumo equations [14], which are a simpler single neuron model than the HH equations. Similar to the case using the HH equations, interesting phenomena, such as extraordinarily slow phase-locked oscillations and the death of all oscillations, are observed. In real systems, internal and external noises fluctuate the biological rhythm. Hence, we also examine the effect of noise on the synchronization and the variability of the interspike intervals. Peculiar phenomena, including noise-induced acceleration and deceleration, are observed.

The rest of this paper is organized as follows: Section 2 presents the mathematical model of a population of globally coupled neuronal oscillators and shows typical oscillations in the system. Section 3 examines the global bifurcation structure and studies the relationship between a slow phase-locked oscillation and the proportion of fast oscillators. Section 4 provides the variability of the interspike intervals in the presence of noise. Finally, Section 5 is the conclusion of this paper. Numerical simulations in this paper are performed using the fourth-order Runge-Kutta method with time step of 0.01.

2. **Rhythmic phenomena in globally coupled neuronal oscillators.**

2.1. **A population of globally coupled neuronal oscillators.**

Herein we consider a population of three-dimensional Bonhoeffer-van der Pol (BVP) or FitzHugh-Nagumo (FHN) oscillators [14] globally coupled through a common buffer (mean field) [7, 21]

$$\frac{dx_i}{dt} = x_i - \frac{{x_i}^3}{3} - y_i - z_i + I_{\text{ext}} + D(w - x_i) + \sigma\xi_i(t), \tag{1a}$$

$$\frac{dy_i}{dt} = \eta(x_i - ay_i), \tag{1b}$$

$$\frac{dz_i}{dt} = \varepsilon_i(x_i - bz_i), \quad \varepsilon_i \ll 1, \tag{1c}$$

$$\frac{dw}{dt} = \frac{D'}{N}\sum_{i=1}^{N}(x_i - w), \quad (i = 1, \cdots, N) \tag{1d}$$

where x_i is the membrane potential, y_i is the refractory variable, and z_i is the (slow) refractory or inhibitory variable of the ith neuronal oscillator. w denotes the common buffer. D and D' represent the coupling strength. The common buffer is a lowpass filtered mean field with a rate constant set by the coupling strength D'. Electrically excitable cells such as neurons and cardiac muscle cells usually interact in pairs through chemical or electrical synapses. The system (1) is considered as a first-order (rough) approximation of these coupled systems. For simplicity, we assume $D \equiv D'$. I_{ext} is the external input current. $\xi_i(t)$ is the white Gaussian noise and σ is the noise intensity. All parameters except I_{ext} are positive. Note that the extended BVP equations are a qualitative neuron model where all variables and parameters are dimensionless.

When $D = 0$ in (1), this system becomes a population of uncoupled extended BVP oscillators. Due to the slow variable z, which is added to the original (two-dimensional) BVP or FHN equations [9, 19], complicated phenomena such as chaos and very slow spiking can be observed [6].

In the following, let the system consist of two kinds of oscillators with different time scales ε_i where

$$\varepsilon_i = \begin{cases} \bar{\varepsilon}_1 & (i = 1, \cdots, M), \\ \bar{\varepsilon}_2 & (i = M+1, \cdots, N), \end{cases} \qquad \bar{\varepsilon}_1 \geq \bar{\varepsilon}_2, \tag{2}$$

and the proportions be $p\,(= M/N)$ and $1 - p$, respectively. ε_i mainly controls the natural period of the oscillator because it is the smallest rate constant among the three variables, although it is difficult to discuss the natural period of such nonlinear oscillators in general. We assume the heterogeneity of natural periods and analyze the dynamics of a population of globally coupled neuronal oscillators. The original (two-dimensional) BVP oscillator with usual parameter values shows the periodic oscillation whose period is about two or three (dimensionless). The introduction of the third variable z with the time scale ϵ may increase the natural period linearly; for example, when $\epsilon = 0.01$, it is increased to the order of several tens. In the coupled system, we expect that phase-locked oscillation whose period is of the same order as the natural period of the single oscillator occurs as the value of D is increased, but in the next section, we show that the unexpected phenomena such as slow phase-locked oscillations and the death of all oscillations are observed.

2.2. **Slow phase-locked oscillations and the death of all oscillations.** In the rest of this subsection and the following section, we consider the system (1) in the absence of noise: $\sigma\xi_i(t) \equiv 0$. Here we show some typical rhythmic phenomena in this system. (Detailed dynamics are discussed in the next section.)

Consider the case when the number of oscillators is ten: $N = 10$. Let $a = 3.0$, $b = 1.0$, $\eta = 0.13$, and $I_{\text{ext}} = -0.4$. If $\bar{\varepsilon}_1 = 0.1$ and $\bar{\varepsilon}_2 = 0.01$, each uncoupled neuronal oscillator shows a simple periodic relaxation oscillation with natural periods of 25 and 168 (dimensionless), respectively. Hereafter, oscillators with $\varepsilon_i = \bar{\varepsilon}_1$ and $\varepsilon_i = \bar{\varepsilon}_2$ shall be referred to as fast and slow oscillators, respectively.

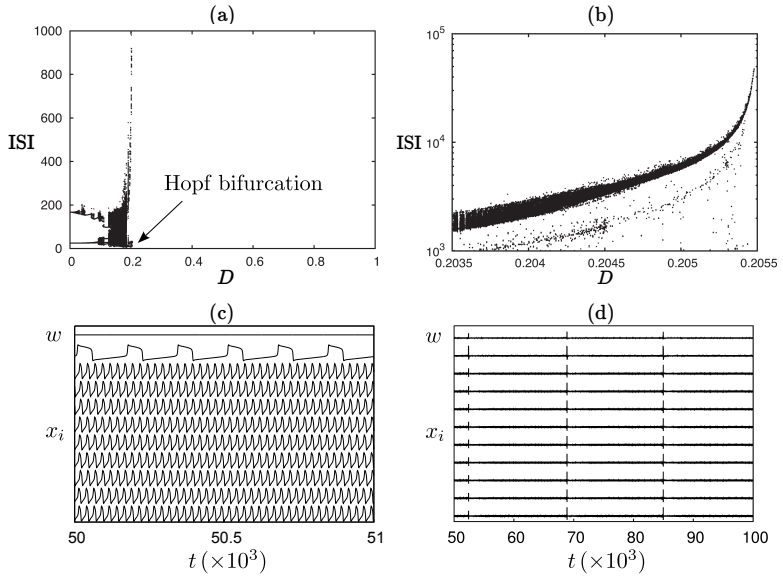

FIGURE 1. (a) Inter-spike intervals (ISIs) vs. coupling strength D. Following a transient of numerical simulations, the ISIs of all oscillators are plotted during $40,000 \leq t \leq 60,000$ for each of the $1,000$ equally spaced D values at the interval $[0, 1]$. (b) Magnification of (a). Scale of the vertical axis is logarithmic. (c), (d) Waveforms of x_i and w when $D = 0$ and $D = 0.2054$, respectively. Each panel denotes the waveforms of x_1, x_2, $\cdots$, x_{10}, and w from the bottom to the top. Scale of the horizontal axis changes between (c) and (d). System consists of nine fast oscillators and one slow oscillator ($p = 0.9$).

Initially we consider a system that consists of nine fast oscillators and one slow oscillator ($p = 0.9$). Figure 1(a) illustrates the interspike-intervals (ISIs) as a function of coupling strength D. Following a transient of numerical simulations, the ISIs of all oscillators are plotted during $40,000 \leq t \leq 60,000$ for each $1,000$ equally spaced D values at an interval of $[0, 1]$. For D values with a few plotted points, oscillators show an almost periodic oscillation, but for D values with many plotted points, they oscillate chaotically. The magnification of this ISIs bifurcation diagram is shown in Fig. 1(b). The ISI value grows up drastically as the value of D increases. Figure 1(c) shows the waveforms of x_i and w when the oscillators are uncoupled ($D = 0$). Each panel denotes the waveforms of x_1, x_2, $\cdots$, x_{10}, and w from the bottom to the top. When the coupling strength is weak, the ISI or the period of such synchronized oscillations is close to a single oscillator's natural period. A slow phase-locked (synchronized) oscillation appears when D is near 0.2 (Fig. 1(d)), and the value of ISI becomes extraordinarily large (greater than 10^4). If the value of D is further increased, the (unique) equilibrium point of the globally coupled system is stabilized and all firings are completely inhibited. Because the period of periodic orbits generated from the Hopf bifurcation is generally small, the slow phase-locked oscillation is an unexpected phenomenon.

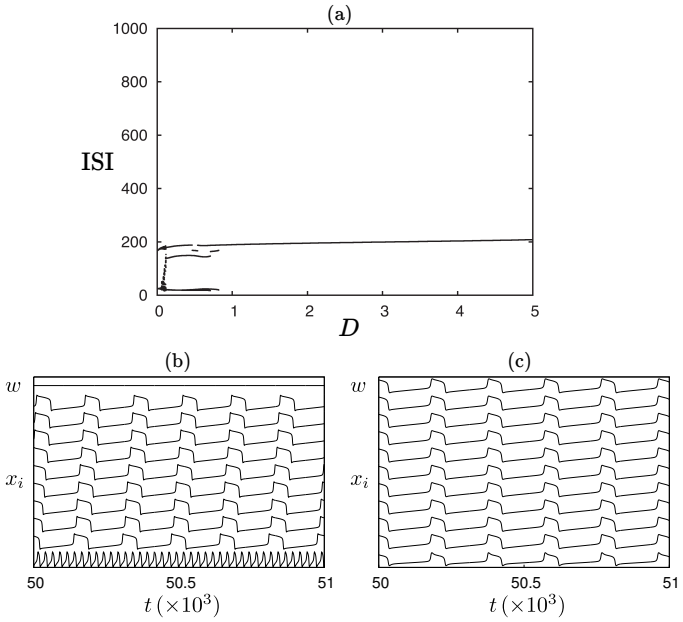

FIGURE 2. (a) Inter-spike intervals (ISIs) vs. coupling strength D. Following a transient of numerical simulations, the ISIs of all oscillators are plotted during $40,000 \leq t \leq 60,000$ for each of the $5,000$ equally spaced D values at the interval $[0, 5]$. (b), (c) Waveforms of x_i and w when $D = 0$ and $D = 2.0$, respectively. Each panel denotes the waveforms of x_1, x_2, $\cdots$, x_{10}, and w from the bottom to the top. System consists of one fast oscillator and nine slow oscillators ($p = 0.1$).

On the other hand, in a system consisting of one fast oscillator and nine slow oscillators ($p = 0.1$), the value of ISI remains fairly constant with coupling strength (Fig. 2(a)). Figure 2(b) shows the waveforms of x_i and w when $D = 0$. Even if the value of the coupling strength is changed, slow synchronization or oscillation death is not observed (Fig. 2(c)).

3. **Relationship between the slow phase-locked oscillation and the proportion of fast oscillators.** In this section, we analyze the local stability of the equilibrium point and the bifurcation structure in the (p, D) plane. Then we examine the relationship between the slow phase-locked oscillation and the proportion of fast oscillators.

3.1. **Local stability of the equilibrium point.** Suppose that a single BVP oscillator has a unique equilibrium point for any value of I_{ext}. If the equilibrium point is $(\bar{x}, \bar{y}, \bar{z})$, then $\bar{x}$ satisfies the following equation,

$$\frac{\bar{x}^3}{3} + \left(\frac{1}{a} + \frac{1}{b} - 1\right)\bar{x} - I_{\text{ext}} = 0. \tag{3}$$

The condition for the uniqueness can be written as

$$\frac{1}{a} + \frac{1}{b} \geq 1. \tag{4}$$

From this uniqueness of the equilibrium point of a single oscillator,

$$\begin{aligned}(x_i, y_i, z_i) &= (\bar{x}, \bar{y}, \bar{z}), \quad (i = 1, \cdots, N)\\ w &= \bar{x},\end{aligned} \tag{5}$$

comes the unique equilibrium point of the coupled system regardless of the value of D. The characteristic polynomial $\Psi(\lambda)$ of the Jacobian matrix at this equilibrium point is

$$\begin{aligned}\Psi(\lambda) = \det &\begin{pmatrix} A_1 & & & & & & d^{\mathrm{T}} \\ & \ddots & & & O & & \vdots \\ & & A_1 & & & & d^{\mathrm{T}} \\ & & & A_2 & & & d^{\mathrm{T}} \\ & O & & & \ddots & & \vdots \\ & & & & & A_2 & d^{\mathrm{T}} \\ d/N & \cdots & d/N & d/N & \cdots & d/N & -D-\lambda \end{pmatrix} \\ &= \{\det(A_1)\}^{Np-1} \cdot \{\det(A_2)\}^{N(1-p)-1} \cdot \det(H),\end{aligned} \tag{6}$$

where

$$d = \begin{pmatrix} D & 0 & 0 \end{pmatrix}, \tag{7}$$

$$A_i = \begin{pmatrix} 1-\bar{x}^2-D-\lambda & -1 & -1 \\ \eta & -a\eta-\lambda & 0 \\ \bar{\varepsilon}_i & 0 & -\bar{\varepsilon}_i b-\lambda \end{pmatrix}, \tag{8}$$

$$H = \begin{pmatrix} A_1 & O & d^{\mathrm{T}} \\ O & A_2 & d^{\mathrm{T}} \\ pd & (1-p)d & -D-\lambda \end{pmatrix}. \tag{9}$$

Although the Jacobian matrix of this system at the equilibrium point is a $(3N+1)\times(3N+1)$ matrix, the analysis of its eigenvalues can be reduced to that of lower dimensional matrices A_i and H [7]. From (6)–(9), it follows that the local stability of the equilibrium point depends on p, $\bar{\varepsilon}_i$, and D, but not on N.

At first, we consider the stability of $\det(A_i)$:

$$\begin{aligned}\det(A_i) = &-\lambda^3 - (a\eta + b\bar{\varepsilon}_i + \bar{x}^2 - 1 + D)\lambda^2 \\ &- \left\{ab\eta\bar{\varepsilon}_i + \eta + \bar{\varepsilon}_i + (a\eta + b\bar{\varepsilon}_i)(\bar{x}^2 - 1 + D)\right\}\lambda \\ &- \eta\bar{\varepsilon}_i\left\{a + b + ab(\bar{x}^2 - 1 + D)\right\}.\end{aligned} \tag{10}$$

Denoting the coefficients of λ^2, λ^1, and λ^0 by $-S_1$, $-S_2$, and $-S_3$, respectively, the condition so that $\det(A_i)$ is stable is given by

$$S_1 > 0 \quad \text{and} \quad S_1 S_2 - S_3 > 0, \tag{11}$$

or

$$S_2 > 0 \quad \text{and} \quad S_1 S_2 - S_3 > 0, \tag{12}$$

since, from (4) we have

$$S_3 = ab\eta\bar{\varepsilon}_i\left(\frac{1}{a} + \frac{1}{b} - 1 + \bar{x}^2 + D\right) > 0. \tag{13}$$

When the coupling strength is sufficiently large, $S_1 > 0$ and $S_2 > 0$ hold. Letting $f(D) := S_1 S_2 - S_3$, $f(D)$ is a quadratic polynomial in D. Since the values of all

parameters except I_{ext} are positive,

$$f(D) = (a\eta + b\bar{\varepsilon}_i)D^2(1 + O(1/D)) > 0. \tag{14}$$

Thus $\det(A_i)$ is stable for $D \gg 1$. On the other hand, if $\det(A_i)$ is unstable at $D = 0$, it is also unstable for $D \ll 1$.

Now we consider the solution of $f(D) = 0$. Calculating the discriminant Δ of $f(D)$, we obtain

$$\Delta = \eta^2(a^2\eta - 1)^2 + 2\eta\bar{\varepsilon}_i(a^2\eta + 1) + O(\bar{\varepsilon}_i^2) > 0. \tag{15}$$

Therefore, $f(D) = 0$ has two distinct real solutions and we define them as D^- and D^+ ($D^- < D^+$).

Solving $S_1 > 0$, $S_2 > 0$, and $f(D) > 0$ gives

$$D > D_1 := -\{a\eta + b\bar{\varepsilon}_i + \bar{x}^2 - 1\}, \tag{16}$$

$$D > D_2 := -\frac{ab\eta\bar{\varepsilon}_i + \eta + \bar{\varepsilon}_i + (a\eta + b\bar{\varepsilon}_i)(\bar{x}^2 - 1)}{a\eta + b\bar{\varepsilon}_i}, \tag{17}$$

$$D < D^-, \quad D^+ < D. \tag{18}$$

From (11), (12), (16)–(18), the condition so that $\det(A_i)$ is stable becomes

$$D > D^+ := \frac{-[\eta\{a^2\eta + 1 + 2a(\bar{x}^2 - 1)\} + O(\bar{\varepsilon}_i)] + \sqrt{\Delta}}{2a\eta + O(\bar{\varepsilon}_i)},$$

because $D^- < D_1\,(D_2) < D^+$. Furthermore, in the singular limit ($\bar{\varepsilon}_i = 0$), this condition becomes

1. The case of $1 - a^2\eta > 0$.

$$D > -\frac{\{1 + a(\bar{x}^2 - 1)\}}{a}. \tag{19}$$

2. The case of $1 - a^2\eta < 0$.

$$D > -(a\eta + \bar{x}^2 - 1). \tag{20}$$

Next, let us consider the stability of $\det(H)$. Because the matrix is 7×7, it is difficult to analytically calculate the region where $\det(H)$ is stable. In the following, the stability of $\det(H)$ is numerically analyzed.

Figure 3 illustrates the region of (p, D) where the equilibrium point is stable. The curves l_1, l_2, and l_3 denote the boundaries of the region where $\det(A_1)$, $\det(A_2)$, and $\det(H)$ are stable respectively. $\det(A_1)$ ($\det(A_2)$) is stable above l_1 (l_2) and unstable below. $\det(H)$ is stable inside l_3 and unstable outside. The region where $\det(A_i)$ is stable includes the region where $\det(H)$ is stable, thus the region where the equilibrium point is stable depends on $\det(H)$, but not on $\det(A_i)$. The equilibrium point is stabilized not through the saddle-node bifurcation but through the Hopf bifurcation, because it is unique for any value of I_{ext} by the assumption (4). The (bold) solid curve l_3 is the Hopf bifurcation curve of the system (1) that denotes the loci of the Hopf bifurcation.

Next, we consider the relationship between the slow phase-locked oscillation and the local stability of the equilibrium point. In Fig. 3, the maximum values of D where a slow phase-locked oscillation occurs are plotted as a cross for each value of p when $N = 25$ ($N = 10$ is too small to analyze the effect of p, thus we increase the number N of the oscillators from 10 to 25). When $p > 0.5$, a slow synchronized oscillation occurs near the Hopf bifurcation. Even in a system that consists only of fast oscillators ($p = 1$), the system oscillates very slowly near $D = 0.2$ and the

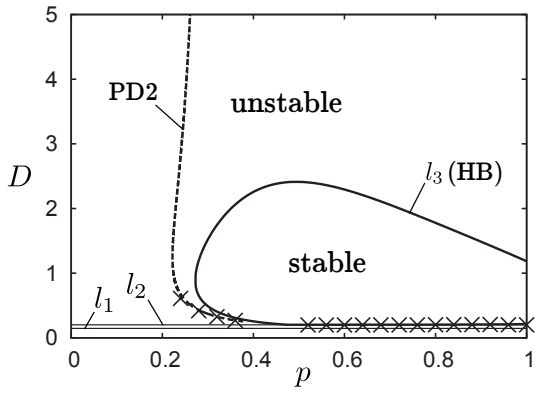

FIGURE 3. Global bifurcation structure in the (p, D) plane. The curves l_1, l_2, and l_3 denote the boundaries of the region where $\det(A_1)$, $\det(A_2)$, and $\det(H)$ are stable respectively. Bold solid curve is the Hopf bifurcation curve of the system (1). Broken curve is the period-doubling bifurcation curve of a reduced system (23). Cross denotes the maximum values of D for each value of p when $N = 25$ where slow phase-locked oscillation occurs.

value of the ISI becomes extraordinarily large (Fig. 4(a)). On the other hand, when $p < 0.22$, the equilibrium point is unstable, and slow synchronization does not appear even if the coupling strength is changed.

When $0.38 < p < 0.5$, slow synchronization does not occur though the Hopf bifurcation occurs in the globally coupled system. We consider a system that consists of four fast oscillators and six slow oscillators ($p = 0.4$). Figure 4(b) shows the ISIs as a function of coupling strength D. If the value of D increases, the population of the oscillators synchronizes or exhibits phase-locked oscillations even though the change in the ISI is negligible. Further increasing the D value completely inhibits the firings.

When $0.22 < p < 0.38$, slow firings occur, but not near the Hopf bifurcation. In particular, when $0.22 < p < 0.27$, the equilibrium point is unstable, and the Hopf bifurcation does not occur even if the D value is changed. In a system that consists of three fast oscillators and seven slow oscillators ($p = 0.3$), a slow synchronized oscillation appears when D is near 0.366 (Figs. 4(c), 4(d)). The range where the ISI value exceeds 10^3 is $0.36596 < D < 0.36603$. In contrast, when $p = 0.9$ (Fig. 1(a)), the range is $0.202 < D < 0.2055$. Thus, for $0.22 < p < 0.38$, a slow phase-locked oscillation occurs in a narrow range compared to $p > 0.5$.

3.2. **The global bifurcation structure.** To analyze the detailed dynamics of globally coupled neuronal oscillators, we examine their bifurcation structure. Here we assume that the system (1) perfectly synchronizes among the same kind of oscillators in the sense that

$$(x_i, y_i, z_i) = (X_1, Y_1, Z_1) \quad (i = 1, \cdots, M), \tag{21}$$

$$(x_i, y_i, z_i) = (X_2, Y_2, Z_2) \quad (i = M + 1, \cdots, N). \tag{22}$$

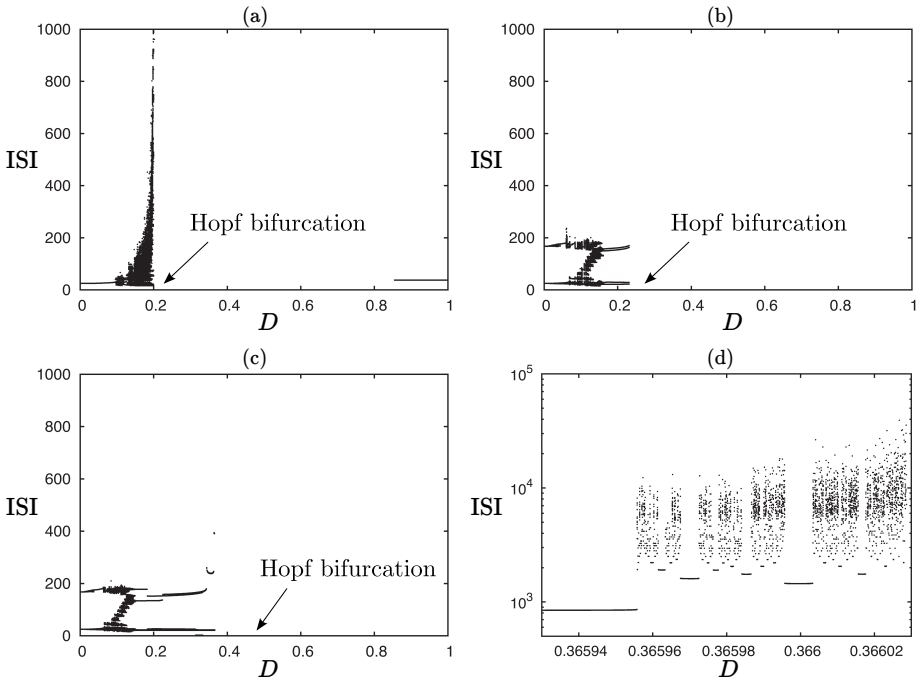

FIGURE 4. Inter-spike intervals (ISIs) vs. coupling strength D. (a) System consists of ten fast oscillators ($p = 1$). (b) System consists of four fast oscillators and six slow oscillators ($p = 0.4$). (c) System consists of three fast oscillators and seven slow oscillators ($p = 0.3$). (d) Magnification of (c). Scale of the vertical axis is logarithmic.

If $w = W$, equation (1) can be reduced to

$$\frac{dX_1}{dt} = X_1 - \frac{{X_1}^3}{3} - Y_1 - Z_1 + I_{\text{ext}} + D(W - X_1), \tag{23a}$$

$$\frac{dY_1}{dt} = \eta(X_1 - aY_1), \tag{23b}$$

$$\frac{dZ_1}{dt} = \bar{\varepsilon}_1(X_1 - bZ_1), \tag{23c}$$

$$\frac{dX_2}{dt} = X_2 - \frac{{X_2}^3}{3} - Y_2 - Z_2 + I_{\text{ext}} + D(W - X_2), \tag{23d}$$

$$\frac{dY_2}{dt} = \eta(X_2 - aY_2), \tag{23e}$$

$$\frac{dZ_2}{dt} = \bar{\varepsilon}_2(X_2 - bZ_2), \tag{23f}$$

$$\frac{dW}{dt} = D\{pX_1 + (1-p)X_2 - W\}, \tag{23g}$$

where all parameters are the same as those in (1). This assumption is satisfied when a slow synchronized oscillation appears. The bifurcation diagram of the reduced model (23) is sufficient for our purpose.

Figure 5 shows the bifurcation diagram of the reduced model (23) as a function of D where the value of X_1 in the steady state is plotted for each value of D.

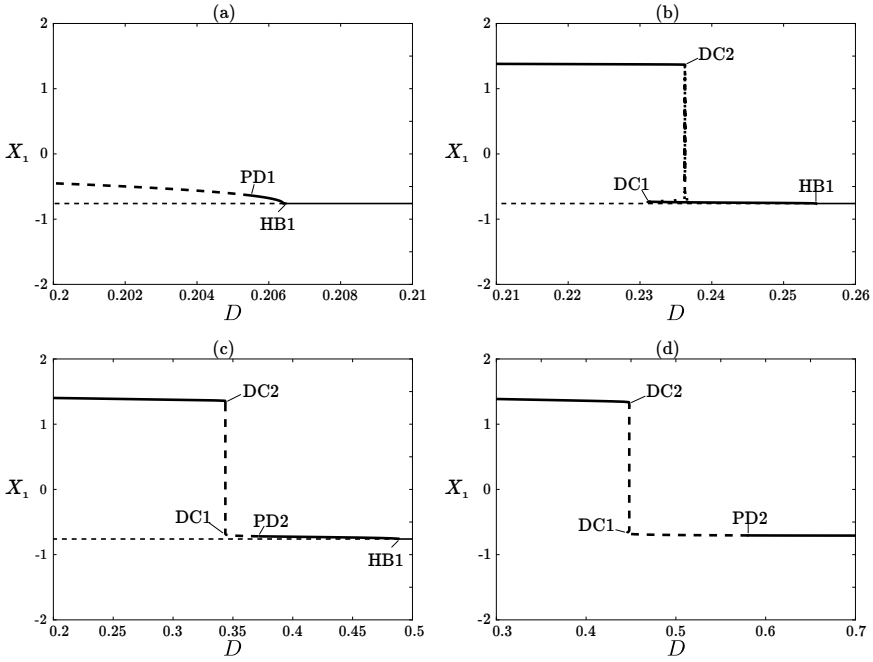

FIGURE 5. One-parameter bifurcation diagram of the reduced model (23) as a function of D. Thin solid and broken curves represent the stable and unstable equilibrium points, respectively. Bold solid and broken curves represent the maximum values of X_1 of the stable and unstable periodic orbits, respectively. HB, PD, and DC (with a number) denote the Hopf bifurcation, period-doubling bifurcation, and double-cycle bifurcation (or saddle-node bifurcation of periodic orbits), respectively. (a) $p = 0.9$. (b) $p = 0.4$. (c) $p = 0.3$. (d) $p = 0.25$.

These diagrams are obtained using the bifurcation analysis software AUTO [4]. The thin solid and broken curves represent the stable and unstable equilibrium points, respectively. The bold solid and broken curves represent the maximum values of X_1 of the stable and unstable periodic orbits, respectively. HB, PD, and DC (with a number) denote the Hopf bifurcation, period-doubling bifurcation, and double-cycle bifurcation (or saddle-node bifurcation of periodic orbits), respectively. When $p = 0.9$ (Fig. 5(a)), a stable periodic orbit is born at the Hopf bifurcation and becomes unstable through the period-doubling bifurcation. Slow synchronization occurs on the left side of PD1. The absence of such simple stable solutions as the equilibrium point or the simple periodic orbit shown in the bifurcation diagram is at least necessary for the occurrence of slow synchronization.

When $p = 0.4$ (Fig. 5(b)), a stable periodic orbit is generated from the Hopf bifurcation. Unlike the case of $p = 0.9$, a double-cycle bifurcation occurs twice. In the range between DC1 and DC2, the system possesses two coexisting stable periodic orbits (one is the periodic orbits with small amplitude between DC1 and HB1, and the other is the periodic orbit with large amplitude on the left side of DC2) at the same parameter value and is bistable. Slow synchronization does not occur

in this case. When $p = 0.3$ (Fig. 5(c)), the global bifurcation structure is similar to Fig. 5(b), but the stable periodic orbit becomes unstable through the period-doubling bifurcation. Slow synchronization appears in the range between PD2 and DC2. When $p = 0.25$ (Fig. 5(d)), the stability of the equilibrium point does not change (data not shown). However, the bifurcation structure of the periodic orbit is similar to Fig. 5(c). Thus, slow firings appear in the range between PD2 and DC2.

The above analyses indicate that the period-doubling bifurcation is important to generate a slow synchronization for $0.22 < p < 0.38$, although we could not clarify how the period-doubling bifurcations affect the slow synchronization. Figure 3 shows the bifurcation curve of PD2 in the (p, D) plane, which is obtained by AUTO. A slow synchronized oscillation occurs near the period-doubling bifurcation for $0.22 < p < 0.38$.

4. **Effect of noise on the synchronization and variability of the interspike intervals.** There have been much work regarding how noise affects the period or frequency of intrinsically oscillating neurobiological systems. The phase oscillator is often employed for examining the noisy nonlinear system analytically [2]. Noise-induced changes in the rhythmic firing activity of the simplest version of a type I neuron or single Hodgkin-Huxley neurons have also been investigated [11, 12, 18]. In particular, the single three-dimensional BVP neuron model indicates various phenomena such as noise-induced acceleration and deceleration [5]. Noise-induced acceleration (deceleration) is the phenomenon that by the introduction of noise neurons come to fire rapidly (slowly) and the ISIs become short (long). In this section, we consider the effect of noise on the synchronization in a population of neuronal oscillators globally coupled through a common buffer and study the variability of the ISIs.

The coefficient of variation (CV) for a random variable T is defined as

$$\mathrm{CV} := \frac{\sqrt{\mathrm{Var}[T]}}{\mathrm{E}[T]}, \tag{24}$$

where $\mathrm{E}[T]$ and $\mathrm{Var}[T]$ are the expectation (mean) and the variance, respectively. CV is dimensionless, and is often used as a measure of the spike train irregularity. If a spike train is regular, $\mathrm{CV} \approx 0$. For a completely irregular spike train like the Poisson process, $\mathrm{CV} = 1$.

In the following, in order to examine the effects of the internal noise, i.e., the fluctuation of ion channels in the membrane of neurons, let the membrane potential x_i be corrupted by noise, as is shown in (1). We consider the case where the system consists of nine fast oscillators and one slow oscillator ($p = 0.9$) and set $D = 0.205$. Figure 6 shows the effect of noise on the slow synchronized firings in the system. Figures 6(a) and 6(b) plot the mean and the CV of the ISIs as a function of noise intensity σ, respectively. Even in the noiseless case ($\sigma = 0$), the value of the ISI is very large and slow synchronization occurs (Fig. 6(c)). As the noise intensity increases, the mean ISI increases drastically and the CV also increases near $\sigma = 0.004$ (Fig. 6(d)). A very small noise decelerates the firing rate of globally coupled neuronal oscillators (noise-induced deceleration). Increasing the noise intensity decreases the mean ISI and reduces the variability (Fig. 6(e)). It should be noted that the noise intensity is not so strong. (See that the waveforms in Fig. 6(f) is not so corrupted by noise.) Further increasing the noise intensity accelerates the firing rate (noise-induced acceleration). The presence of noise leads to non-monotonic (average) period or frequency as the noise intensity increases.

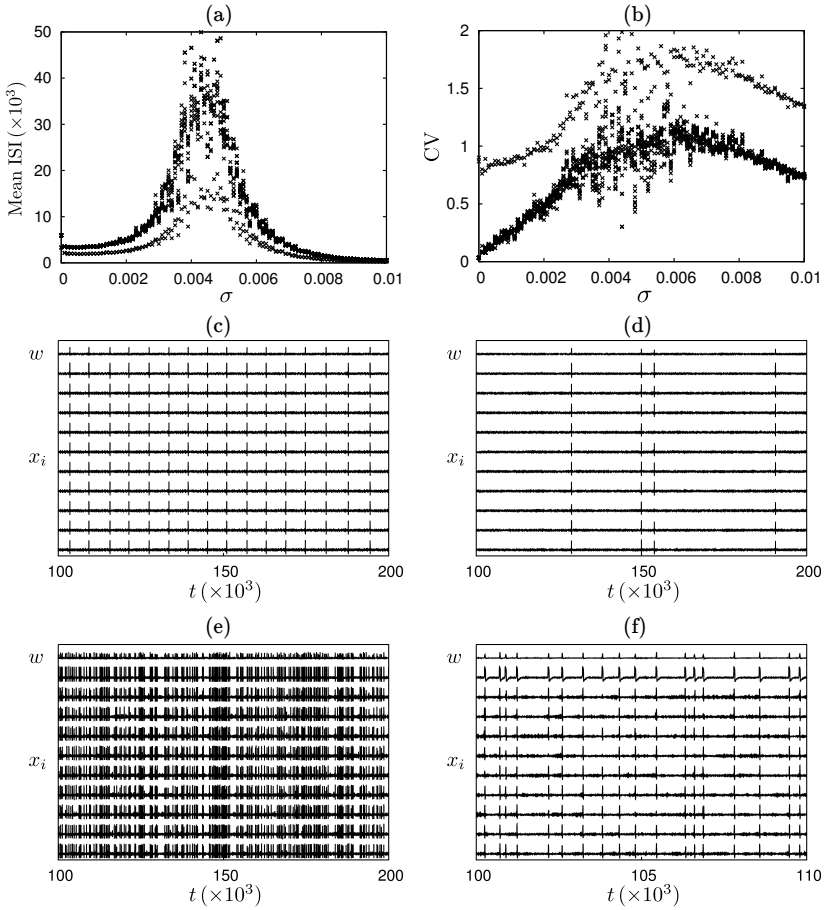

FIGURE 6. Effect of noise on the slow phase-locked oscillation. System consists of nine fast oscillators and one slow oscillator ($p = 0.9$). $D = 0.205$. (a) Mean ISI vs. noise intensity σ. (b) CV vs. noise intensity σ. (c), (d), (e) Waveforms of x_i and w when $\sigma = 0$, $\sigma = 0.004$, and $\sigma = 0.01$, respectively. (f) Magnification of (e). Each panel denotes the waveforms of x_1, x_2, $\cdots$, x_{10}, and w from the bottom to the top.

These phenomena can be observed in the single BVP oscillator and its dynamics in the presence of noise is quite similar to the coupled system. More detailed analyses on the coupled system in the presence of noise are necessary to clarify whether noise-induced phenomena peculiar to the coupled system exist or not.

5. **Conclusion.** A population of extended BVP or FHN oscillators globally coupled through a common buffer (mean field) exhibits interesting phenomena, such as a very slow synchronization and the death of all oscillations. To determine the detailed dynamics of a globally coupled system, we examined the global bifurcation structure. The dynamics can be classified into four groups by the proportion of fast oscillators (Fig. 3).

- $p > 0.5$: Slow synchronization occurs near the Hopf bifurcation of the globally coupled system (Figs. 1 and 5(a)). It appears even in a system with only fast oscillators (Fig. 4(a)).
- $0.38 < p < 0.5$: Although slow synchronization does not occur, the Hopf bifurcation does (Figs. 4(b) and 5(b)).
- $0.22 < p < 0.38$: Slow synchronization occurs not near the Hopf bifurcation but near the period-doubling bifurcation (Figs. 4(c), 4(d), 5(c), and 5(d)).
- $0 < p < 0.22$: Slow synchronization does not occur, and the equilibrium point is unstable even if the coupling strength is changed (Fig. 2).

Slow synchronization appears when $p > 0.5$ and $0.22 < p < 0.38$. However, the generation mechanisms differ because the bifurcation structures are different and for $0.22 < p < 0.38$ the range where slow firings can occur is much narrower compared to $p > 0.5$. The slow phase-locked oscillation is an unexpected phenomenon because the period of periodic orbits generated from the Hopf bifurcation is usually small. This suggests the existence of a global bifurcation such as the homoclinic bifurcation (note that the equilibrium point of the coupled system is unique for all values of parameters, thus the homoclinic orbit is not the usual one of a saddle equilibrium point, but maybe the Shilnikov-type one or the homoclinic orbit to a saddle-type periodic orbit), or some kind of period-doubling cascade. In particular, when $0.22 < p < 0.38$, it seems that the period-doubling cascade leads to the extraordinarily slow oscillation because it occurs near the period-doubling bifurcation. However, the detailed mechanism is not clear and this is a future subject.

In addition, we examined the effect of noise on the synchronization and the variability of the interspike intervals. Similar to the single extended BVP oscillator, peculiar phenomena such as noise-induced acceleration and deceleration are observed. This indicates that a very small noise may greatly influence the biological rhythm and seems related to stochastic resonance in the period. However, it seems difficult to clarify this mechanism even for the reduced model (23), and thus more elaborated studies are necessary.

Acknowledgments. We would like to thank the referees very much for their valuable comments and suggestions to improve our original manuscript. This work was partially supported by the Japan Society for the Promotion of Science (No. 245002-74), and the Aihara Project, which is the FIRST program from JSPS initiated by CSTP.

REFERENCES

[1] R. Borisyuk, D. Chik and Y. Kazanovich, *Visual perception of ambiguous figures: Synchronization based neural models*, Biol. Cybern., **100** (2009), 491–504.
[2] L. Cheng and B. Ermentrout, *Analytic approximations of statistical quantities and response of noisy oscillators*, Physica D, **240** (2011), 719–731.
[3] H. Daido, *Why circadian rhythms are circadian: Competitive population dynamics of biological oscillators*, Phys. Rev. Lett., **87** (2001), 048101.
[4] E. J. Doedel and B. E. Oldeman, et al., *AUTO-07P: Continuation and bifurcation software for ordinary differential equations*, Concordia University, 2009.
[5] S. Doi and J. Inoue, *Chaos and variability of inter-spike intervals in neuronal models with slow-fast dynamics*, AIP Conf. Proc., **1339** (2011), 210–221.
[6] S. Doi and S. Kumagai, *Generation of very slow neuronal rhythms and chaos near the Hopf bifurcation in single neuron models*, J. Comp. Neurosci., **19** (2005), 325–356.
[7] S. Doi and S. Sato, *Regulation of differentiation in a population of cells interacting through a common pool*, J. Math. Biol., **26** (1988), 435–454.

[8] B. Ermentrout and M. Wechselberger, *Canards, clusters, and synchronization in a weakly coupled interneuron model*, SIAM J. Appl. Dyn. Syst., **8** (2009), 253–278.
[9] R. FitzHugh, *Impulses and physiological states in theoretical models of nerve membrane*, Biophy. J., **1** (1961), 445–466.
[10] L. Glass, *Synchronization and rhythmic processes in physiology*, Nature, **410** (2001), 277–284.
[11] B. Gutkin and B. Ermentrout, *Dynamics of membrane excitability determine interspike interval variability: A link between spike generation mechanisms and cortical spike train statistics*, Neural Comput., **10** (1998), 1047–1065.
[12] B. Gutkin, J. Jost and H. Tuckwell, *Inhibition of rhythmic neural spiking by noise: The occurrence of a minimum in activity with increasing noise*, Naturwiss., **96** (2009), 1091–1097.
[13] A. L. Hodgkin and A. F. Huxley, *A quantitative description of membrane current and its application to conduction and excitation in nerve*, J. Physiol., **117** (1952), 500–544.
[14] J. Honerkamp, G. Mutschler and R. Seitz, *Coupling of a slow and a fast oscillator can generate bursting*, Bull. Math. Biol., **47** (1985), 1–21.
[15] G. Katriel, *Synchronization of oscillators coupled through an environment*, Physica D, **237** (2008), 2933–2944.
[16] H. Kori, Y. Kawamura and N. Masuda, *Structure of cell networks critically determines oscillation regularity*, J. Theor. Biol., **297** (2012), 61–72.
[17] Y. Kuramoto, "Chemical Oscillations, Waves, and Turbulence," Springer Series in Synergetics, **19**, Springer-Verlag, Berlin, 1984.
[18] B. Lindner, A. Longtin and A. Bulsara, *Analytic expressions for rate and CV of a type I neuron driven by white Gaussian noise*, Neural Comput., **15** (2003), 1761–1788.
[19] J. Nagumo, S. Arimoto and S. Yoshizawa, *An active pulse transmission line simulating nerve axon*, Proc. IRE, **50** (1962), 2061–2070.
[20] A. Pikovsky, M. Rosenblum and J. Kurths, "Synchronization: A Universal Concept in Nonlinear Sciences," Cambridge Nonlinear Science Series, **12**, Cambridge University Press, Cambridge, 2001.
[21] K. Sugimoto, Y. Nii, S. Doi and S. Kumagai, *Frequency variability of neural rhythm in a small network of pacemaker neurons*, Proc. of AROB 7th '02, (2002), 54–57.

Received December 15, 2012; Accepted July 05, 2013.

E-mail address: tneki716@rotary.kuee.kyoto-u.ac.jp
E-mail address: doi@kuee.kyoto-u.ac.jp
E-mail address: jdoi@mail.koka.ac.jp